Computers and Concrete, Vol. 9, No. 4 (2012) 245-255
DOI: http://dx.doi.org/10.12989/cac.2012.9.4.245

Simulation of the damping effect of a high-rise CRST frame structure

Xilin Lu[1], Hongmei Zhang*[1] and Chunguang Meng[2]

[1]*State Key Laboratory of Disaster Reduction in Civil Engineering, Tongji University, Shanghai, 200092, China*
[2]*Architecture Design & Research Institute of Tongji University, Shanghai 200092, China*

(Received April 30, 2010, Revised May 16, 2011, Accepted June 22, 2011)

Abstract. The damping effect of a Concrete-filled Rectangular Steel Tube (CRST) frame structure is studied in this paper. Viscous dampers are employed to insure the function of the building especially subjected to earthquakes, for some of the main vertical elements of the building are not continuous. The shaking table test of a 1:15 scale model was conducted under different earthquake excitations to recognize the seismic behavior of this building. And the vibration damping effect was also investigated by the shaking table test and the simulation analysis. The nonlinear time-history analysis of the shaking table test model was carried out by the finite element analysis program CANNY. The simulation model was constructed in accordance with the tested one and was analyzed under the same loading condition and the simulation effect was then validated by the tested results. Further more, the simulation analysis of the prototype structure was carried out by the same procedure. Both the simulated and tested results indicate that there are no obvious weak stories on the damping equipped structure, and the dampers can provide the probability of an irregular CRST frame structure to meet the requirements of the design code on energy dissipation and deformation limitation.

Keywords: concrete-filled rectangular steel tube; high-rise building; viscous damper; shaking table test; nonlinear time-history analysis.

1. Introduction

A CRST structure is constructed by steel beams and columns of Concrete-filled Rectangular Steel Tube (CRST). The deformation ductility of a CRST structure can be improved due to the interaction of the concrete and steel. The inner concrete of a CRST element is surrounded by the steel tube, and the lateral deformation can be confined under vertical pressure, so the concrete compressive strength can be improved (Starossek *et al.* 2010). On the other hand, the inner concrete can prevent the steel tube from easily instable and buckling which is help to improve the seismic prevention ability. Therefore, the CRST element is often recommended to use in high-rise structures (Jiang *et al.* 2009).

The research work on a Concrete-filled Rectangular Steel Tubular frame structure has been introduced to clarify and improve the seismic prevention ability in this paper. To gain more space and the architectural effect, some of the columns of the structure are taken off. Since the main vertical element is not continuous, the viscous dampers are considered to equipped on this building. The viscous dampers can provide larger damping, and the stiffness of the structure can not be changed obviously, which

* Corresponding author, Associate professor, Ph. D., E-mail: zhanghongmei@tongji.edu.cn

may reduce the vibration effectively without changing the structural arrangement or increasing the dimensions of structural member. For the above reasons, the viscous dampers are employed to the CRST frame structure. The main vertical structural members of this building are arranged like the character “L” and are rotated to go up. The arrangement may induce large torsional response of the whole structure or weak locations in the structure.

Although damper equipped structure is suggested, the damping effects still remain vague. In order to evaluate the damping effect, the nonlinear time history analysis of the high-rise CRST frame structure with dampers is carried out. The nonlinear time-history simulation for the shaking table test model (1:15) of the structure is performed by the finite element program-CANNY and compared with the shaking table model test. The simulation analysis for the prototype structure is also performed in this investigation to evaluate the damping effect of the real project. Deformation effect and energy dissipation effect is mainly investigated.

2. Structure description

2.1 Overview of the structure

The high-rise building analyzed in this investigation is a 21-storey CRST frame structure located in Shanghai with 56 viscous dampers fixed on it. It is 49 m by 49 m in plane with an overall height of 100 m. The slabs of two floors are L-shaped and one is square which turns 90 degrees every three floors from bottom to top. This kind of slab distribution induces many slender columns without lateral support of slabs in three-floor height. For this reason, dampers are employed to brace the columns rotating along with the structure. The typical plane views and the typical elevation view are shown in Figs. 1(a) and (b) respectively.

2.2 Distribution plan of the dampers

The damping force F can be expressed as Eq (1),

$$F = c\ \mathrm{sgn}(\dot{u})|\dot{u}|^{\alpha} \tag{1}$$

Where c is damping coefficient, sgn ( ) is the signum function, $\dot{u}$ means the relative velocity of the two ends of the damper and α stands for the velocity index.

The dynamic equation of the structure can be expressed as Eq. (2)

$$[M]\{\ddot{x}\}+[C]\{\dot{x}\}+[K]\{x\} = -[M]\{\ddot{x}_g\} \tag{2}$$

Here, $[M]$, $[C]$, $[K]$ stand for the mass matrix, damping matrix and rigidity matrix respectively. $\{\ddot{x}\},\{\dot{x}\},\{x\}$ represent the acceleration vector, velocity vector and displacement vector respectively and $\{\ddot{x}_g\}$ is the ground acceleration vector.

According to the characters of the dampers, the viscous damper can be adjusted to provide damp with no rigidity, and the mass can also be ignored. If this kind of dampers is fixed on the original structure, the structure dynamic function can be described as Eq. (3)

$$[M]\{\ddot{x}\}+([C]+[C_d])\{\dot{x}\}+[K]\{x\} = -[M]\{\ddot{x}_g\} \tag{3}$$

Here, C_d is the additional damp matrix which may influence the solution of the function, including the acceleration, velocity and displacement. To get more optimum structural distribution plan, the location, number and property of the dampers should be adjusted according to the structural characteristic and design request.

In order to investigate the seismic behavior, the simulation analysis of the damping effect based on the shaking table model test which was conducted in the State Key Laboratory of Disaster Reduction in Civil Engineering in Tongji University, Shanghai, China was carried out. The dynamic characteristics, seismic response, especially the effect of the dampers on seismic behaviors of the building are investigated.

The arrangement of the dampers was subjected to the conditions of architectural restriction, and the dampers can only be adjusted in a limited scope because of the type, dimension and other limitations of the dampers. Here, the damping coefficient c is set as 250 kN/(mm·s^{-1})$^{\alpha}$, and the velocity index α is set as 0.15. The maximum damping force can be controlled within 500 kN, or else the outer shape of the damper will be too large for the building. The responses of the structure using the adopted damper arrangement are verified to meet the request of the code (GB 50011-2001).

3. Shaking table model test

3.1 Construction of the model

The target investigated structure is a 1:15 scale model structure. The main columns are constructed by steel rectangular tube and filled with concrete. According to the similarity relationship, the material property of the model should have low elastic modulus and high gravity. Besides, the stress-strain relationship of the model material should be similar to the prototype material. Under this consideration, micro concrete and copper are selected to simulate the concrete and steel of the prototype structure respectively. The design principle of the model damper is to keep same property to the prototype damper and the size of the model damper should be small enough to be installed onto the model structure. The main similarity relationship is listed in Table 1.

The velocity index of the damper of the model structure is maintained as 0.15 and the damping coefficient c is set as 0.3 kN/(mm·s^{-1})$^{\alpha}$.

The model structure was constructed in the State Key Laboratory of Disaster Reduction in Civil Engineering of Tongji University. The copper tubes were located and fixed on the base firstly, and then the copper beams were welded on the copper tube columns from lower to higher floor. After all beams of the constructing floor were welded, the wires were pasted on the beams and then the micro concrete was poured to form the slab. When all floors were constructed, the micro concrete was poured into the copper tube columns. Finally, the braces and the dampers were fixed on the model corresponding to the original structure. The whole model is 6.7 m in height including the base and 19t in weight including additional mass blocks and the base. The three dimension diagram and the picture of the shaking table model are shown in Figs. 1(c) and (d) respectively.

Table 1 Main similarity relationship of the model structure

Physical parameter	Dimension	Elastic modulus	Mass	Time	Frequency	Acceleration	Force
Similarity relationship	1:15	1:5	1:3375	1:6.708	6.708:1	3:1	1:1125

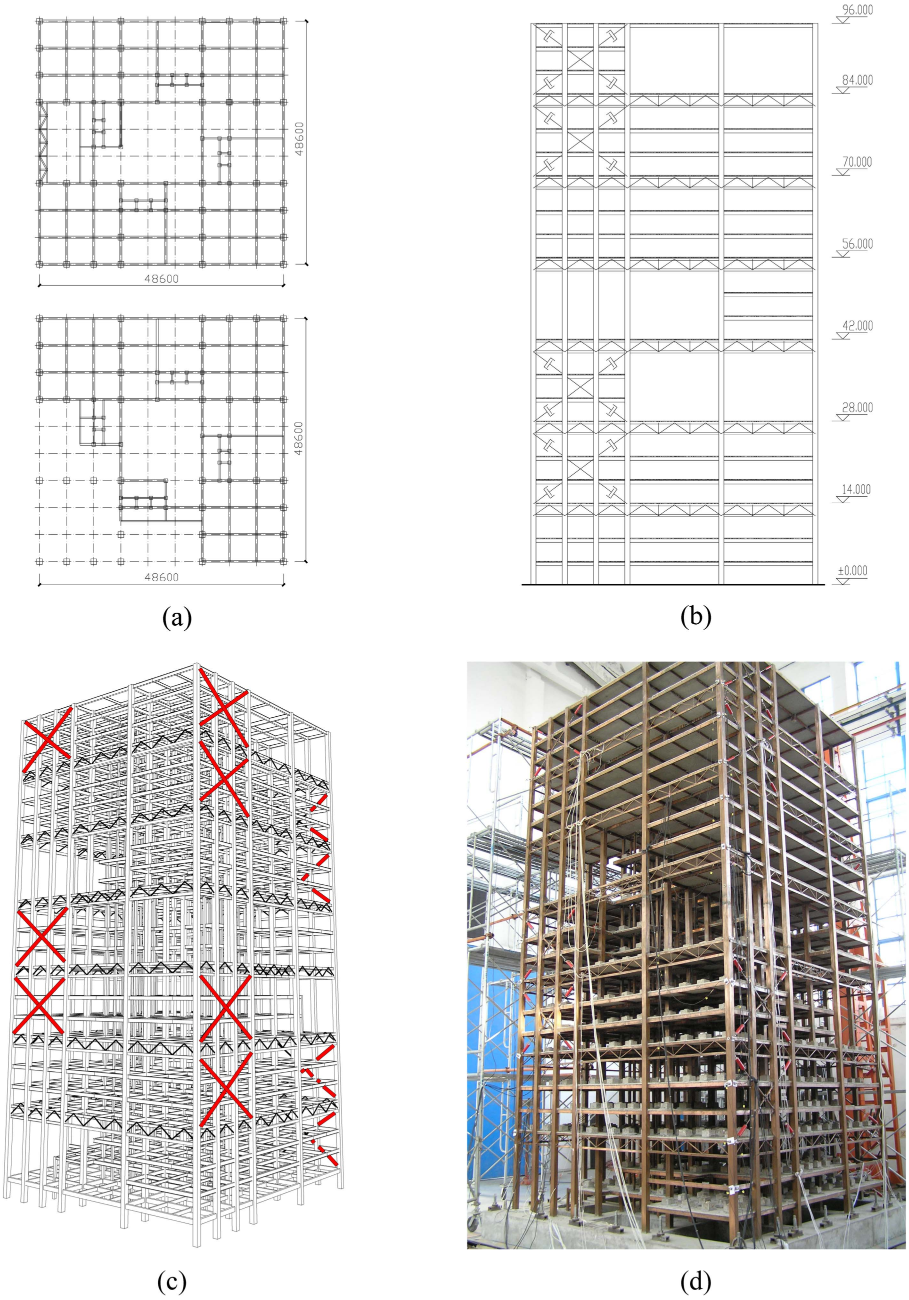

Fig. 1 Overview of the shaking table model: (a) typical construction plan, (b) elevation view, (c) three dimension view of the structure and distribution plan of the dampers, (d) picture of the shaking table model

3.2 Test program

The shaking table model test was carried out on MTS shaking table of the State Key Laboratory of Disaster Reduction in Civil Engineering in Tongji University. The structural model and loading program were designed according to the law of similarity. El Centro, Pasadena and the second Shanghai artificial earthquake waves were selected as the input excitation. The similarity of the acceleration was set as 3:1. The peak acceleration value of the earthquake wave was adjusted to 110gal, 300gal, 660gal and 1200gal respectively corresponding to 35gal, 100gal, 220gal and 400gal for the prototype structure (GB 50011-2001 2001). The input wave was exerted in two directions for those with the peak acceleration of 110gal, 300gal and 660gal. And only one direction was set for the wave with the peak acceleration of 1200gal due to the capacity limitations of the shaking table equipment. For the 110gal seismic excitation, tests were conducted respectively before and after the dampers were installed on the structural model. The damping effect on the seismic response of the structure was investigated by the shaking table tests. The peak acceleration of the input seismic excitation and the input direction are shown in Table 1. The white noise test was conducted before and after each of the above defined test cases to identify the frequency, mode shapes and damping ratio of the structural model.

Three types of sensors were fixed at appropriate positions of the structure model. Eight displacement sensors were used to record the displacement response of the key floors. Thirty five acceleration sensors were employed to record the acceleration response of different floors. Among 24 strain gages, 16 were located on the key lateral force resisting members and 8 were on the connecting bars of the dampers so that to get the damping force and the energy dissipation information of the dampers.

4. Nonlinear time-history analysis

4.1 Analysis model

In this nonlinear analysis, the computational program CANNY was employed to investigate the damping effect of the target structure. The beams and columns of the structural analysis model were constructed with multi-spring element, and the floor was supposed to be rigid here (Park and Kim 2008). The multi-spring element (MS model) (Li *et al.* 2000) was selected to simulate the CRST columns and the steel beams as shown in Fig. 2(a). This kind of MS element has two internal nodes, and its two ends allow the interactions of biaxial bending moments and the varying axial

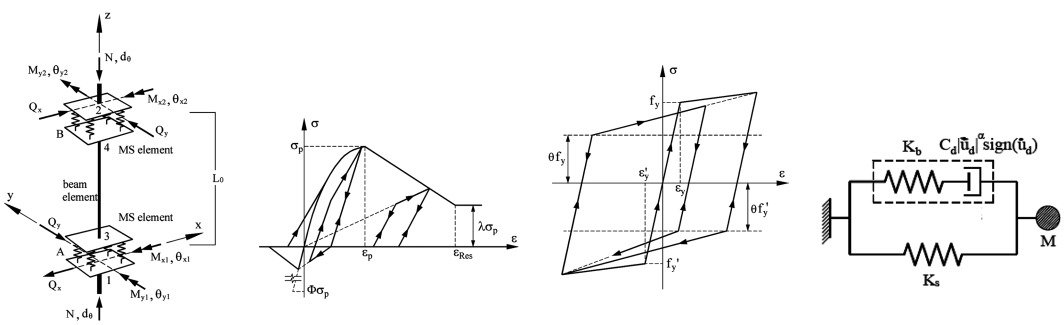

(a) (b) (c) (d)

Fig. 2 Analysis model: (a) multi-spring element, (b) concrete stress-strain constitutive relationship, (c) steel bar stress-strain constitutive relationship, (d) damper element load on the element (Hu *et al.* 2010). As for CRST columns, the uniaxial concrete stress-strain constitutive relationship used in the MS model allows the confine effect of the steel tube to the concrete (Li *et al.* 2000). The concrete constitutive relation is shown in Fig. 2(b). Bilinear model was used as the steel bar stress-strain constitutive relationship (Sabri *et al.* 2009), which is shown in Fig. 2(c). The damper model in this analysis was adopted the damper model of the CANNY program. The parameters of the dampers were defined by the property of the applied dampers (Kato and Miyajima 2009) (De *et al*. 2010). The damper element has a dashpot in force-velocity relationship or a combination of dashpot and spring (Ghosh and Spanos 2009) (Kavianipour and Sadati 2009) (Kounadis 2009), and the springs can reflect the stiffness properties of the dampers. The applied damper element was composed with a dashpot and a spring in serial connection, as shown in Fig. 2(d). The stiffness-proportional damping can be made to the initial stiffness and/or the instantaneous stiffness. Also special kind of element, damping element (or damper) can be used to represent any device that resists the relative velocity between two points in the structural model. The relative property of the dampers was collected from the damper element test in Tongji University.

4.2 Dynamic property analysis

The tested and simulated values of the initial natural period of this model structure are shown in Table 2. Besides the results of CANNY analysis model, the analysis results of ETABS model with the elastic deformation assumption of the floor were also presented here. As the table demonstrates, the simulated results agree with the test results well except for the third natural cycle (the third natural period of the tested result is also an approximate value due to the testing accuracy). The results in Table 2 indicate that the dynamic characteristic of the tested model can be simulated by the adopted analysis elements and model especially in the elastic stage.

4.3 Failure development

During the test procedure, there was no apparent damage found when the excitation was 110gal. When the input excitation intensity was 300gal, large spacing and tiny out-of-plane deformation appeared at many bottom chords of the belt trusses between the columns. When the input excitation was 1200gal, the middle and bottom parts of the model structure were seriously damaged. There were large spacing buckle at the bottom chords of many belt trusses and many of them were out-of-plane damage. The oblique web members of most of the belt trusses between the columns had visible spacing buckle or yield deformation. Besides, three braces on the 8th and 11th floor were yield also. The simulated results also see the weak locations in the model of the building which is consistent with the test results.

Table 2 Natural periods of the model structure (unite: *s*)

Model No.	First	Second	Third	Fourth	Fifth	Sixth	Seventh	Eighth
CANNY	0.663	0.649	0.473	0.213	0.208	0.153	0.115	0.111
ETABS	0.637	0.634	0.489	0.210	0.206	0.157	0.113	0.112
Tested	0.614	0.614	0.341	0.207	0.207	0.146	0.105	0.102

4.4 The damping effect

The shaking table model was tested under the selected earthquake waves which were adjusted according to the design code in China. Since El Centro, Pasadena earthquake waves are considered as the typical earthquake input excitation to cause notable damage and Shanghai artificial earthquake wave is the typical local earthquake wave, these three earthquake waves were selected as the input excitation in the shaking table test. Furthermore, the structural response under Shanghai artificial earthquake wave was selected to investigate the damping effect for its local property and can present closer damage and other response information of the prototype structure. Under the different excitation intensity of SHW2 earthquake wave, time history curve of the roof displacement are shown in Figs. 3~5. As observed, good agreement between analysis and tested time history curve of the roof displacement is obtained for the model structure without dampers when the input acceleration is 110gal. As for the curves of structure with dampers, the curve on the early stage agrees with each other well, but the simulated result appears faster than the tested one at the latter

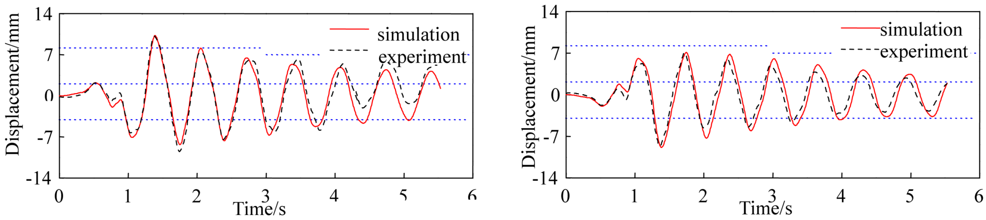

(a) Main input direction—X (b) Main input direction—Y

Fig. 3 The top displacement response under the 2nd Shanghai artificial earthquake wave-peak acceleration: 110gal (without dampers)

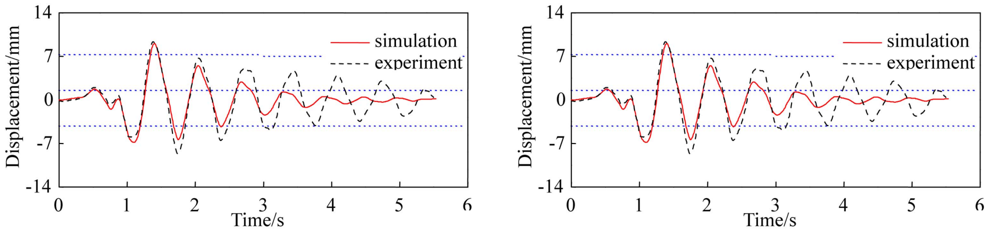

(a) Main input direction—X (b) Main input direction—Y

Fig. 4 The top displacement response under the 2nd Shanghai artificial earthquake wave-peak acceleration: 110gal (with dampers)

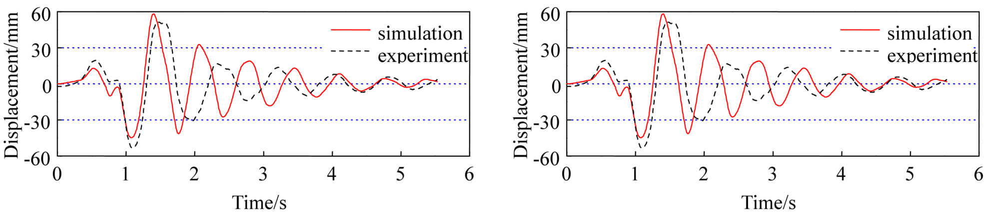

(a) Main input direction—X (b) Main input direction—Y

Fig. 5 The top displacement response under the 2nd Shanghai artificial earthquake wave-peak acceleration: 660gal (with dampers) test procedure. It indicates that the energy dissipation effect of damper of the simulation is better than that of the test. This may attribute to the size of the model dampers. And another reason may contribute to the tiny deformation which is no lager than the existing clearance in the ball joints and prevents the dampers come into play. With the increasing of the seismic excitation, the effect of the connecting clearance in the ball joints became weak and the simulated result became consistent with the tested one. In general, the simulated results can represent the properties of this reduced scale model.

From Fig. 3 and Fig. 4, it can be observed that the top displacement of the model reduces after the viscous dampers were fixed, especially at the later stage of the time history excitation procedure. This kind of damper is a velocity viscous damper which is sensitive to velocity, and the weak rigidity will not affect the rigidity of the original structure apparently. It can provide additional damping when the structure is experiencing a vibration excitation such as earthquake action. The viscous will come into play when it is excited by an initial excitation, and it will not take effect when the initial excitation is too weak. The energy dissipation effect will increase with the excitation velocity is speed up until the damping equipment lose efficacy.

The comparison between the model structures with and without dampers was performed when the peak excitation was 110gal. The target model structure without dampers was tested under the peak earthquake excitation of 110gal first, and then, this model structure was fixed with the special dampers and was excited with the same intensity earthquake input. At the start testing few seconds, the displacement time history curve was almost same in both directions. After the initial one or two seconds, the amplitude of the displacement value was greatly reduced by the installation of the dampers. Since the viscous damper needs an initial velocity to take effect, it is understandable for the initial delay of the damping effect.

For the limitation of the experiment condition, the target model structure can only be tested as damper installed structure after the excitation of 110gal. The displacement time history curve presented in Fig. 5 demonstrates that the amplitude of the displacement is reduced fast under the input excitation of 660gal, which can be evidenced by the tested results and the simulated results. There still exists difference between the tested results and simulated results, which may also caused by the installation error.

5. Dynamic responses of prototype structure

As above stated, the simulated results agree with the tested results well. There still exists difference between the tested and simulated results, and the reason can be attributed to the construction error. The applied simulation model is constructed by multi-spring element and the damper element which is used to simulated the properties of beams/columns and dampers respectively. Since testing conditions are limited to make a full scale experiment, the simulation analysis is considered as an effective reference to comprehend the real structure. Using the same simulation elements, the simulation analysis for prototype structure was performed by the same procedure to investigate the damping effect of the full scale structure.

The first two natural frequencies of the prototype structure are 0.246Hz and 0.253Hz, corresponding to the translational motion. Under the excitation intensity of 35gal, the maximum elastic inter-storey drift is 1/527 in Y direction and 1/504 in X direction, which meet the requirement of the code (1/300) for elastic response of frame structures. And the maximum nonlinear inter-story drift is 1/98 in

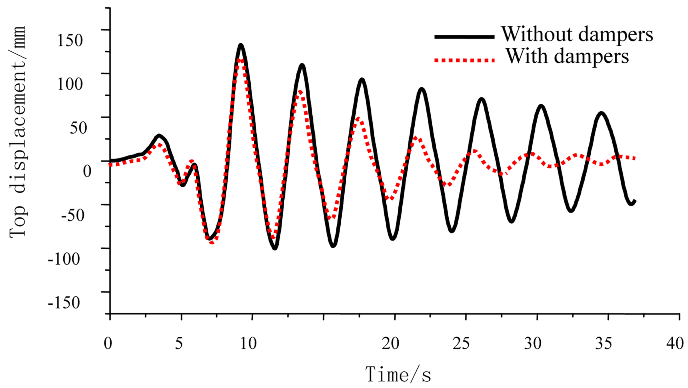

Fig. 6 The prototype displacement time history curve-excitation: 35gal (SHW2)

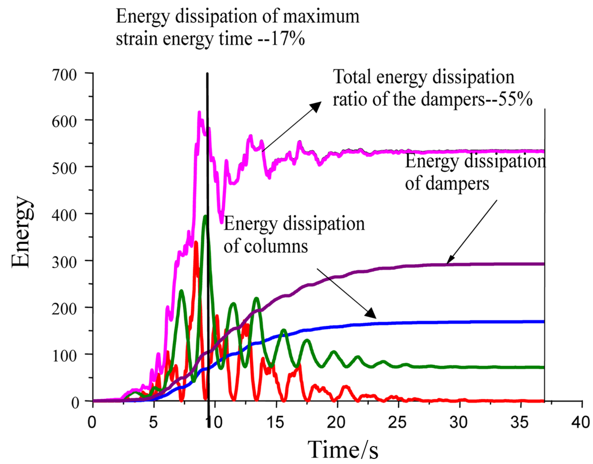

Fig. 7 Energy dissipation time history curve-excitation: 35gal (SHW2)

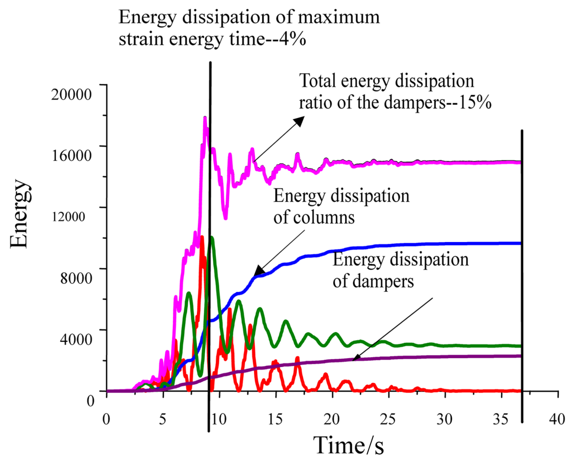

Fig. 8 Energy dissipation time history curve-excitation: 220gal (SHW2)

Y direction and 1/91 in X direction under the excitation of 220gal, which still meet the requirement of the code (1/80) for energy dissipation frame structures. The displacement time history curve is shown in Fig. 6 when the excitation is 35gal, and it can be observed that the displacement is greatly reduced for the function of the dampers after the initial excitation. The damping effect will play a role after it is waked up by an initial excitation, and the dampers will serve as the energy dissipation element so the deformation will be reduced during this sequence.

The simulation energy dissipation results are shown in the energy dissipation time history curves presented in Fig. 7 and Fig. 8. Each time history curve represents the energy dissipation value of a kind of structure element and the envelope curve represents the whole energy dissipation. It can be observed that the energy dissipation value of the dampers reaches 55% of the total energy dissipation when the input excitation is 35gal. And the energy dissipation ratio of the dampers is 17% at the time of the maximum strain energy dissipation moment. The energy dissipation ratio of the dampers is 15% of the total energy dissipation when the input excitation reaches 220gal. And the energy dissipated by the dampers is 4% at the time of the maximum strain energy dissipation moment.

The peak excitations of 35gal and 220gal of the earthquake wave represent the conventional and rare earthquake input in China code of certain site and certain design seismic intensity respectively. Both the experimental and simulated results indicate that the damping effect is notable when the input excitation is 35gal, and the energy dissipation value of the dampers to the total energy dissipation becomes weakened under the excitation of 220gal. The beams, columns and other structure members play a more important role at the larger excitation stage. The beams, columns and other structure members come into its plastic stage with the amplification of the input excitation. And the plastic deformation dissipates most of the earthquake energy. So the ratio of the damping effect is weakened at this stage and the actual value may different due to the arrangement, the number and the type of the dampers applied in the structure. Since the analyzed high-rise CRST frame structure is satisfied with the requirement of the bearing capacity and displacement ductility, most of the energy can be dissipated by the main structure members of the CRST columns and the dampers as demonstrated in Fig. 7 and Fig. 8.

6. Conclusions

To sum up, the dynamic behavior of the dampers fixed onto the high-rise CRST frame structure is investigated by the shaking table model test and the simulation analysis. The simulation model analysis in this research provided acceptable time history results comparing to the experimental one. The dampers take effect after the initial excitation is overcome and can reduce the amplitude of the deformation. The damping effect is notable under the excitation of conventional input intensity, and the energy dissipation ratio becomes weakened when the input earthquake is increased to rare earthquake intensity. These results are drawn under the target analysis CRST frame structure and the optimize plan can be designed considering the tested and simulated behavior of the dampers.

Acknowledgements

The authors are grateful for the financial support of the National Science Foundation of China (Grant No. 90815029, 51008226), Kwang-Hua Fund for College of Civil Engineering in Tongji University and National Key Technology R&D Program (Grant No. 2006BAJ13B01) of China.

References

De Pasquale, G., Veijola, T. and Soma, A. (2010), “Modeling and validation of air damping in perforated gold and silicon MEMS plates”, *J. Micromech. Microeng.*, **20**(1), 1-12.

Ghosh, R. and Spanos, P.D. (2009), “Determination of offshore spar stochastic structural response accounting for nonlinear stiffness and radiation damping effects”, *J. Mech. Mater. Struct.*, **4**(7-8), 1327-1340.

Hu, H.T., Su, F.C. and Elchalakani, M. (2010), “Finite element analysis of CFT columns subjected to pure bending moment”, *Steel Compos. Struct.*, **10**(5), 415-428.

Jiang, H.J., Lu, X.L. and Kubo, T. (2009), “Maximum displacement profiles of reinforced concrete frames”, *J. Asian Arch. Build. Eng.*, **8**(2), 183-190.

Kato, D., Miyajima, Y. and Nakamura, Y. (2009), “Evaluating method of deformation at losing point of axial

load carrying capacity of RC columns", *J. Asian Arch. Build. Eng.*, **8**(2), 501-508.
Kavianipour, O. and Sadati, S.H. (2009), "Effects of damping on the linear stability of a free-free beam subjected to follower and transversal forces", *Struct. Eng. Mech.*, **33**(6), 709-724.
Kounadis, A. (2009), "The Effect of infinitesimal damping on neoconservative divergence instability systems", *J. Mech. Mater. Struct.*, **4**(7-8), 1415-1428.
Li, K.N., Kubo, T., Ventura, C. and Yang, S.T. (2000), "3D Analysis of building model and reliability of simulated structural earthquake responses", *Build. Struct.*, **30**, 14-18.
Ministry of Construction of the People's Republic of China. (2001), Code for seismic design of buildings (GB 50011-2001) (English Version), China.
Park, J.W. and Kim, S.E. (2008), "Nonlinear inelastic analysis of steel-concrete composite beam-columns using the stability functions", *Struct. Eng. Mech.*, **30**(6), 763-785.
Sabri, F., Lakis, A.A. and Toorani, M.H. (2009), "Hybrid finite element method in supersonic flutter analysis of circular cylindrical shells", *31st International Conference on Boundary Elements and other Mesh Reduction Methods*, New Forest England.
Starossek, U., Falah, N. and Lohning, T. (2010), "Numerical analyses of the force transfer in concrete-filled steel tube columns", *Struct. Eng. Mech.,* **35**(2), 241-256.

CC